Berylliumlike Mo XXXIX and lithiumlike Mo XL observed in the Joint European Torus tokamak

B. Denne, G. Magyar, and J. Jacquinot
JET Joint Undertaking, Abingdon, OXON OX14 3EA, United Kingdom
(Received 5 May 1989)

The resonance lines of berylliumlike and lithiumlike molybdenum have been observed in high-temperature Joint European Torus tokamak discharges into which molybdenum was introduced using the laser blow-off method. The measured transition wavelengths are $2s^2\,{}^1S_0-2s2p\,{}^1P_1$ 49.904±0.03 Å, $2s^2\,{}^1S_0-2s2p\,{}^3P_1$ 137.787±0.03 Å for Mo XXXIX, and $2s\,{}^2S_{1/2}-2p\,{}^2P_{1/2}$ 143.998±0.02 Å, $2s\,{}^2S_{1/2}-2p\,{}^2P_{3/2}$ 58.499±0.02 Å for Mo XL. For the berylliumlike ion the results are compared with the semiempirical predictions by Edlén [Phys. Scr. **28**, 51 (1983)], while the results for lithiumlike Mo are compared with the calculations by Johnson, Blundell, and Sapirstein [Phys. Rev. A **37**, 2764 (1988)].

I. INTRODUCTION

The study of highly ionized, high-Z elements is of interest for spectroscopic diagnostics of the high-temperature plasmas that are found in modern tokamaks such as the Joint European Torus (JET) and the Tokamak Fusion Test Reactor (TFTR). Molybdenum ($Z=42$), in its Be- and Li-like ionization stages, is suitable for diagnosing plasmas with central electron temperatures in the range 6–10 keV.

Further, accurate determination of the transition wavelengths for the resonance lines of few-electron systems such as the Be- and Li-like ions of high-Z elements is of fundamental interest in atomic physics, where such measurements can be compared to precise theoretical calculations or semiempirical predictions. Thus Johnson *et al.*[1] have pointed out that for the Li sequence there is a small but significant discrepancy between experimental values and calculations including one-electron quantum electrodynamics (QED) contributions, which they have attributed to screening of the Lamb shift. For the Be-sequence resonance lines, Denne and Hinnov[2] have noted a systematic deviation from the semiempirical predictions by Edlén[3] in the range $Z=28-36$: the singlet line wavelengths become increasingly longer and the intercombination line wavelengths shorter than predicted with increasing Z. Tokamak plasmas with high carbon concentrations (as is the case for both JET and TFTR) provide good possibilities for accurate measurements since the carbon lines emitted are strong and high grating orders of the C V and C VI resonance lines are easily observable, and may thus be used as references.

II. EXPERIMENT

The target plasmas were and 3- and 5-MA deuterium discharges into which molybdenum was introduced using the recently installed JET laser blow-off system.[4] In addition to the Ohmic heating, several MW of ion-cyclotron resonance heating (ICRH), in the hydrogen minority scheme, were admitted for supplementary heating. The central electron temperature was in the range 9.2–10.4 keV, and the central electron density ranged from 2.8 to 3.7×10^{13} cm^{-3} for the 3-MA discharges, whereas the corresponding parameters for the single 5-MA discharge used were 7.6 keV and 6.3×10^{13} cm^{-3}, respectively.

Spectra were recorded using a 2-m extreme-grazing-incidence Schwob-Fraenkel spectrometer,[5] equipped with a 600-groove/mm grating, and two microchannel-plate image intensifier-converter detector systems, fiber-optically coupled to 1024-element photodiode arrays. The detectors, moveable along the Rowland circle, cover 20–60 Å portions of spectrum, depending on wavelength. The spectral resolution (full width at half maximum) is ~0.2 Å. The nominal spectral range of the instrument is (approximately) 15–340 Å. In the present experiment, however, scans were restricted to regions covering the four resonance lines, and in first grating order only, due to a lack of machine time.

In Fig. 1 is shown the ~49–59-Å region before (dashed line) and after (solid line) molybdenum injection. The Mo XXXIX $2s^2\,{}^1S_0-2s2p\,{}^1P_1$ and Mo XL $2s\,{}^2S_{1/2}-2p\,{}^2P_{3/2}$ transitions are seen along with part of the C VI Lyman series in second grating order. These carbon lines were used as wavelength references, along with C VI L_α in second order (at 67.4720 Å) and the C V resonance and intercombination lines at 40.2683 (Ref. 6) and 40.7306 Å, respectively. For the two long-wavelength molybdenum lines (around ~140 Å), again C V and C VI lines (in high orders) were used as references, as well as nickel lines (nickel being an intrinsic impurity in JET). For the wavelength determination, spectral data were integrated for 164 msec, while, in order to obtain the temporal evolution of the molybdenum lines with adequate time resolution, scans were made with 16-msec integration time. Figure 2 shows the time histories of the Mo XXXII 127.868-Å line (Na-like) and the Li-like Mo XL line at 143.998 Å. Both lines have been normalized to their peak values; on an absolute scale, the Mo XL signal is about 20 times smaller than the Mo XXXII signal—hence the much higher level of noise in the former signal. The molybdenum injection takes place at 7.5 sec into the discharge, as indicated in the figure. During the time depicted in Fig. 2, the electron density remains constant.

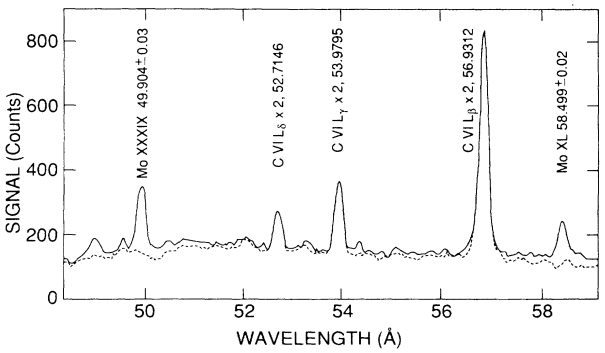

FIG. 1. Spectrum in the region ~49–59 Å before (dashed line) and after (solid line) injection of molybdenum.

The central electron temperature, also shown in Fig. 2, is on the average constant, but exhibits sawtoothlike behavior, caused by a magnetohydrodynamic instability of the plasma. It is seen in Fig. 2 that the Mo XL line peaks considerably later (~250 msec) than the Mo XXXII line, confirming the behavior expected of a much higher ionization stage. (The immediate early peak just after 7.5 sec may be attributed to a blending line of a low ionization stage of Mo, or a momentary change in the background plasma, associated with the injection.) The drop to a lower level of the Mo XL signal at ~8 sec is presumably caused by the sawtooth crash in the temperature at this time, leading to an expulsion of Mo from the plasma center. A corresponding increase in signal for the Mo XXXII line may be seen at the same time, this ion being located radially further out in the plasma (where the temperature is essentially unchanged). The Mo XL signal recovers to a lower level after the crash, and a further drop can be seen at the time of the next sawtooth crash, at ~8.4 sec, although less pronounced.

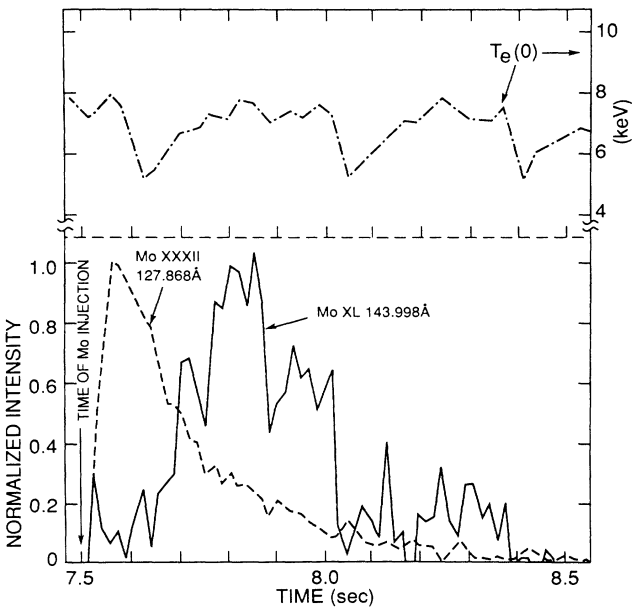

FIG. 2. Time evolution of the Mo XXXII 127.868-Å (Na-like) and the Li-like Mo XL line at 143.998 Å. Also shown (top) is the central electron temperature, $T_e(0)$.

For the wavelength determination, the positions of the molybdenum lines and the reference lines were established. A weighted, least-squares fit of the references was made using orthogonal (Chebyshev) polynomials. Generally, a fourth-order polynomial provided the best fit. The wavelengths of the Mo lines were subsequently determined. This process was repeated for the several individual scans, and the final wavelengths, given below, were obtained by taking an average of the individual measurements. The error limits were estimated from the spread of the individual results for each molybdenum line and were conservatively set so as to cover all the individual results.

As mentioned earlier, measurements were performed in first grating order only. The two long-wavelength lines could, in principle, be measured in second order, within the wavelength range covered by the spectrometer. To improve on the relative accuracy of measurement of the two short-wavelength transitions, higher-order observations would be desirable, although in some higher orders, line blending will be a problem. (For example, the second order of the Mo XL $2s\,^2S_{1/2}-2p\,^2P_{3/2}$ transition will fall in the wing of the strong resonance line of Mg-like Mo XXXI at 116.0 Å.)

III. RESULTS

The wavelengths obtained are 49.904±0.03 and 137.787±0.03 Å for the Mo XXXIX resonance and intercombination lines, respectively, while for Mo XL, the results are 58.499±0.02 and 143.998±0.02 Å for the $2s\,^2S_{1/2}-2p\,^2P_{3/2}$ and $2s\,^2S_{1/2}-2p\,^2P_{1/2}$ transitions, respectively. The corresponding energy level values are presented in Table I. Also given are the calculated energies by Johnson *et al.*[1] for Li-like Mo and the semiempirical predictions by Edlén[3] for Be-like Mo. Regarding Li-like Mo XL we shall here merely state that the observed deviation between experiment and theory is consistent with an observation in Kr (Ref. 7) and further down in the sequence. This deviation is attributed to a screening of the Lamb shift.[1] For a detailed discussion of the lithium sequence we would like to refer to a recent paper by Hinnov and Denne *et al.*[6] For the beryllium se-

TABLE I. Energy levels (in cm^{-1}) of Mo XXXIX and Mo XL.

Spectrum	Level	Experimental energy	Predicted energy
Mo XXXIX	$2s^2\,^1S_0$	0	0
	$2s2p\,^3P_1$	725 758±158	722 026[a]
	$^1P_1$	2 003 847±1200	2 009 300[a]
Mo XL	$2s\,^2S_{1/2}$	0	0
	$2p\,^2P_{1/2}$	694 454±96	715 788[b]
	$^2P_{3/2}$	1709 430±585	1 729 001[b]

[a]Reference 3 (extrapolated).
[b]Reference 1 (interpolated).

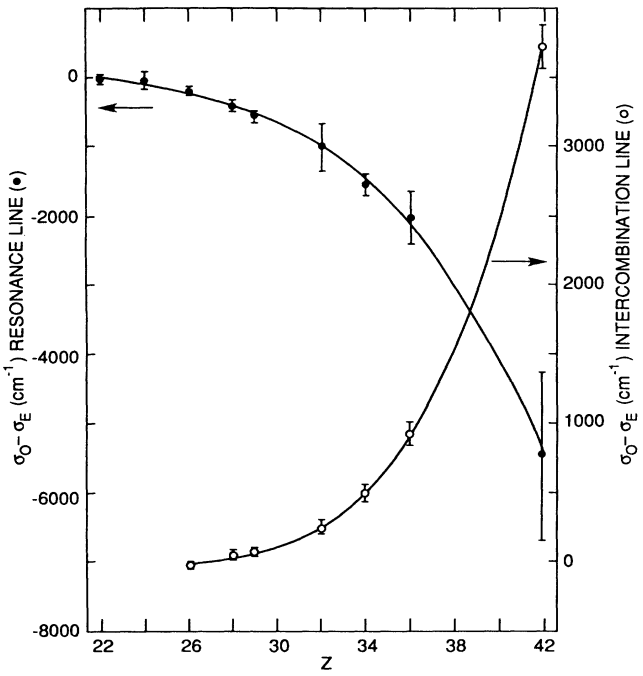

FIG. 3. Difference between observed wave number (σ_O) and predicted by Edlén (σ_E) for the Be-sequence resonance line (filled circles) and intercombination line (open circles) in the range $Z=22-42$. The graphs are least-squares polynomial fits to the respective data points.

quence resonance and intercombination lines, the present observations in Mo XXXIX confirm the systematic deviation from the semi-empirical predictions by Edlén[3] as observed further down in the sequence by Denne and Hinnov.[2] The difference between observed wave number, and predicted by Edlén, is illustrated in Fig. 3 for the resonance and intercombination lines for the range $Z=22-42$. The experimental wavelengths are given in Tables II and III for the $2s^2\,{}^1S_0-2s2p\,{}^1P_1$ and $2s^2\,{}^1S_0-2s2p\,{}^3P_1$ transitions, respectively. In order to obtain the predicted wave numbers for elements beyond krypton, the formulas given in Ref. 3, Tables V and VI, were extrapolated. It is seen from the figure that the resonance line wavelength is becoming increasingly longer than predicted (lower wave number), while the intercombination line wavelength is becoming increasingly shorter. In this context, it is interesting to note that the $^1S_0$-$^3P_1$ transition wavelength eventually becomes shorter than the $^2S_{1/2}$-$^2P_{1/2}$ resonance line of the lithiumlike ion—this takes place near $Z=31$. In Cu ($Z=29$) the Cu XXVI $^1S_0$-$^3P_1$ line and the Cu XXVII $^2S_{1/2}$-$^2P_{1/2}$ line are at 227.808 and 224.795 Å (Ref. 8), respectively, while in Ge ($Z=32$) the said transitions are at 199.36 (Ref. 9) and 200.290 Å (Ref. 6), respectively.

The deviation from Edlén's predictions is attributed to the lack of accurate data beyond Ni ($Z=28$) at the time (1983), and furthermore poor or conflicting measurements, particularly for iron and nickel. Since then, not only have measurements been extended to higher Z, but more precise measurements have become available for Fe

TABLE II. Observed wavelength (λ_o) and wave number (σ_o) for the $2s^2\,{}^1S_0-2s2p\,{}^1P_1$ transition of the Be sequence for elements in the range $Z=22-42$. σ_E is the wave number predicted by Edlén, and λ_c is the wavelength obtained from the graph in Fig. 3.

Z	Spectrum	λ_o (Å)	σ_o (cm^{-1})	σ_E (cm^{-1})	λ_c (Å)
22	Ti XIX	169.585±0.02[a]	589 675±70	589 710	169.572
23	V XX			627 555	159.362
24	Cr XXI	149.90±0.03[b]	667 111±135	667 166	149.913
25	Mn XXII			708 759	141.126
26	Fe XXIII	132.913±0.01[b]	752 372±57	752 574	132.920
27	Co XXIV			798 863	125.227
28	Ni XXV	117.995±0.01[a]	847 494±72	847 894	117.996
29	Cu XXVI	111.186±0.01[b]	899 394±81	899 954	111.180
30	Zn XXVII			955 349	104.744
31	Ga XXVIII			1 014 397	98.659
32	Ge XXIX	92.90±0.03[a]	1 076 426±350	1 077 432	92.898
33	As XXX			1 144 793	87.444
34	Se XXXI	82.285±0.010[b]	1 215 288±150	1 216 835	82.280
35	Br XXXII			1 293 933	77.390
36	Kr XXXIII	72.756±0.02[c]	1 374 457±380	1 376 480	72.761
37	Rb XXXIV			1 464 876	68.383
38	Sr XXXV			1 559 524	64.245
39	Y XXXVI			1 660 847	60.337
40	Zr XXXVII			1 769 281	56.651
41	Nb XXXVIII			1 885 280	53.176
42	Mo XXXIX	49.904±0.03[d]	2 003 847±1200	2 009 300	49.904

[a]Reference 2.
[b]Reference 8.
[c]Reference 7.
[d]Present work.

TABLE III. As in Table II for the $2s^2\,{}^1S_0-2s2p\,{}^3P_1$ transition for elements in the range $Z=26-42$.

Z	Spectrum	λ_o (Å)	σ_o (cm^{-1})	σ_E (cm^{-1})	λ_c (Å)
26	Fe XXIII	263.755±0.01[a]	379 140±20	379 164	263.738
27	Co XXIV			398 737	250.777
28	Ni XXV	238.83±0.02[b]	418 708±35	418 653	238.836
29	Cu XXVI	227.808±0.01[a]	438 966±19	438 896	227.808
30	Zn XXVII			459 443	217.604
31	Ga XXVIII			480 273	208.144
32	Ge XXIX	199.360±0.03[c]	501 605±75	501 362	199.360
33	As XXX			522 686	191.190
34	Se XXXI	183.580±0.02[d]	544 722±60	544 223	183.580
35	Br XXXII			565 948	176.480
36	Kr XXXIII	169.845±0.025[e]	588 772±87	587 844	169.846
37	Rb XXXIV			609 899	163.635
38	Sr XXXV			632 091	157.812
39	Y XXXVI			654 410	152.345
40	Zr XXXVII			676 845	147.202
41	Nb XXXVIII			699 390	142.357
42	Mo XXXIX	137.787±0.03[f]	725 758±158	722 026	137.787

[a]Reference 8.
[b]Reference 2.
[c]Reference 9.
[d]Reference 10.
[e]Reference 7.
[f]Present work.

and Ni. The most reliable and up-to-date experimental data to our knowledge are listed in Tables II and III, and have been used in the comparison with Edlén's values. A weighted, least-squares fit of a polynomial in Z has been made to the difference between observed and predicted wave numbers for both the resonance and the intercombination line. The fitted graphs are shown in Fig. 3. From the graphs we may obtain recalculated wavelengths to be compared with the measurements, as well as interpolated wavelengths for elements not yet investigated. Wavelengths thus obtained are given in the rightmost column of Tables II and III. The accuracy of the recalculated wavelengths is estimated to be ±0.02 Å, or better.

The semiempirical predictions by Edlén[3] were based on multiconfiguration Dirac-Fock calculations by Cheng, Kim, and Desclaux.[11] If we compare the observed wave numbers with those of Cheng *et al.* in the Z range shown in Fig. 3, we find that for the singlet line, the theoretical wave numbers are too low by about 0.3% throughout (i.e., the calculated wavelengths are too long). For the intercombination line, the theoretical wave numbers are too low by about 0.2% at Ni, and become too high for higher Z (about 0.15% at $Z=42$) compared to the observed values. In view of the experimental accuracy now attainable, more accurate theoretical calculations are called for for the beryllium sequence, preferably on a par with those by Johnson *et al.* for the lithium isoelectronic sequence, although we appreciate the greater theoretical complexity associated with the presence of one more electron in the case of the berylliumlike ion.

ACKNOWLEDGMENTS

The authors wish to thank Dr. E. Hinnov for several fruitful discussions. The enthusiastic support of this experiment by the JET Operating Team, in particular Dr. M. Bures, Dr. P. Lallia, and Dr. P. Nielsen, is gratefully acknowledged.

[1]W. R. Johnson, S. A. Blundell, and J. Sapirstein, Phys. Rev. A **37**, 2764 (1988).
[2]B. Denne and E. Hinnov, Phys. Scr. **35**, 811 (1987).
[3]B. Edlén, Phys. Scr. **28**, 51 (1983).
[4]G. Magyar, M. R. Barnes, S. Cohen, A. Edwards, N. C. Hawkes, D. Pasini, and P. J. Roberts, JET Report No. JET-R(88)15, 1988.
[5]J.-L. Schwob, A. W. Wouters, S. Suckewer, and M. Finkenthal, Rev. Sci. Instrum. **58**, 1601 (1987).
[6]E. Hinnov and the TFTR Operating Team, and B. Denne and the JET Operating Team, Phys. Rev. A (to be published).
[7]B. Denne, E. Hinnov, J. Ramette, and B. Saoutic, Phys. Rev. A **40**, 1488 (1989).
[8]E. Hinnov (private communication).
[9]E. Hinnov, F. Boody, S. Cohen, U. Feldman, J. Hosea, K. Sato, J.-L. Schwob, S. Suckewer, and A. Wouters, J. Opt. Soc. Am. **B3**, 1288 (1986).
[10]E. Hinnov, A. Ramsey, B. Stratton, S. Cohen, and J. Timberlake, J. Opt. Soc. Am. B **4**, 1293 (1987).
[11]K. T. Cheng, Y.-K. Kim, and J. P. Desclaux, At. Data Nucl. Data Tables **24**, 111 (1979).